Journal of Sound and Vibration (2002) **254**(5), 849–865
doi:10.1006/jsvi.2001.4128, available online at http://www.idealibrary.com on IDEAL®

AXISYMMETRIC VIBRATIONS OF CONCENTRIC DISSIMILAR ORTHOTROPIC COMPOSITE ANNULAR PLATES

J. B. Greenberg and Y. Stavsky

Faculty of Aerospace Engineering, Technion—Israel Institute of Technology, Haifa 32000, *Israel.*
E-mail: ystavsky@aerodyne.technion.ac.il

(*Received* 10 *May* 2001)

The axisymmetric vibrational behaviour of two concentric dissimilar orthotropic composite annuli is investigated. Sixth order systems of equations of motion for each annulus are presented together with the matching conditions at their interface. The common frequency of vibration of the structure is determined numerically using a finite difference method. Bi-layered, triple-layered and bi- + triple-layered material compositions were considered. Computed results for a wide range of possible orthotropic material combinations indicate the complex role the material orthotropies play in determining the annuli's vibrational response. It is shown that the *frequency increase factor* (defined as the ratio between the highest and lowest frequencies obtained for all inner and outer material combinations considered) is very sensitive to the geometric, heterogeneity and orthotropy parameters of the composite annular plates. Unfortunately, no simple rule of thumb formula for estimating the effect of the material composition on the frequency appears to be deducible. However, in keeping with previous results for concentric dissimilar *isotropic* annuli, the geometry (expressed via the radii of the inner and outer annuli) and the different material compositions were found to exert a considerable influence on the natural frequency of vibration. In the absence of appropriate analytical expressions, optimization and, thereby, control of the natural frequency of composite plate-like structures, through geometry and material composition, must make use of parametric studies similar to the current one.

1. INTRODUCTION

The problem of vibrations of composite plates is of great importance in the context of aerospace and mechanical engineering applications. The heterogeneity of the plates is almost exclusively considered in the thickness direction. Thus, for example, Stavsky and Loewy [1] presented a closed-type solution for axisymmetric vibrations of circular plates laminated from various isotropic materials. This work was extended by Greenberg and Stavsky [2] to the case of axisymmetric vibrations of polar orthotropic layered plates. Recently, Lin and Tseng [3] have tackled the problem of free vibrations of polar orthotropic laminated circular and annular plates using a first order shear deformation theory and a finite element solution (see also relevant references quoted therein).

However, there is practical engineering interest in the behaviour of multi-annular plates. Frostig and Simitses [4] investigated the buckling of multi-annular plates. Each of the isotropic, homogeneous plates was permitted to have its own geometry or material properties. The plates were subjected to axisymmetric in-plane forces, either at the outer

0022-460X/02/$35.00

edge or at one of the circumferential joints or a combination of the two. Numerical results were presented for two-part plates, indicating the influence of the different properties of the annular parts. Lee [5] analyzed the buckling of annular plates with stepped variation in thickness using a numerical method based on the Rayleigh principle. The plates were single-layered, isotropic and consisted of the same material. The influence of the thickness ratio of the various concentric plates on the compressive buckling load was computed.

An allied problem was considered by Gorman [6] who investigated the transverse vibrational frequencies of polar orthotropic annular plates of variable thickness using the finite element method.

More recently, Greenberg and Stavsky [7] examined a situation in which each concentric annulus was laminated of different isotropic materials giving rise to heterogeneity in both the thickness and radial directions. A closed-type solution was found from which the natural frequency of vibration could be extracted. It was found that for certain combinations of material lay-ups higher frequencies of vibration could be achieved than for an equivalent single plate structure. In addition, altering the radius-to-thickness ratio of the inner plate could optimize the higher frequencies. The extensive computed results provided an insight into the main factors that influence, and can therefore be potentially used to control, the natural frequencies of vibration. The popularity of composite materials in aerospace structures, due to their high strength-to-weight ratio, motivates the current work. In this paper, the scope of reference [7] is broadened to consider concentric dissimilar *orthotropic* composite plates undergoing axisymmetric vibrations.

2. FORMULATION OF THE PROBLEM

2.1. STRAIN–DISPLACEMENT RELATIONS

Consider two concentric annular plates of equal thickness h. Properties of the inner and outer plates will be denoted by superscripts I and O respectively. Let b and c be the inner and outer radii of the inner plate, respectively, and c and a the inner and outer radii of the outer plate (see Figure 1). Both plates are composed of orthotropic materials with elastic properties that are thickness dependent. The compositions of the two plates are permitted to be different from each other. Following Kirchhoff's hypothesis the strain–displacement relations, in each plate, are

$$\varepsilon_r = u', \qquad \varepsilon_\theta = u/r, \tag{1}$$

where the prime denotes differentiation with respect to r. The radial, circumferential and transverse displacements are, respectively, taken to be

$$u(r, z, t) = u_0(r, t) + z\beta, \quad v(r, z, t) = 0, \quad \omega(r, z, t) = w_0(r, t), \tag{2}$$

where z is the thickness co-ordinate and β is the change of slope in the radial direction. As a consequence, the strains are expressed as linear functions of z:

$$(\varepsilon_r, \varepsilon_\theta) = (\varepsilon_{r0}, \varepsilon_{\theta 0}) + z(\kappa_r, \kappa_\theta). \tag{3}$$

The in-plane radial and circumferential reference strains, at $z = 0$, are given by

$$\varepsilon_{r0} = u_0', \qquad \varepsilon_{\theta 0} = u_0/r, \tag{4}$$

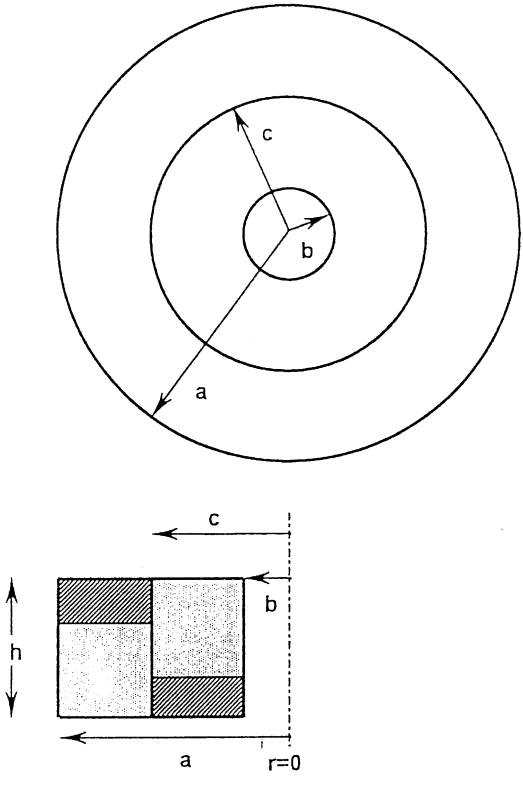

Figure 1. Composite concentric dissimilar orthotropic annuli.

whereas the corresponding plate curvatures are given in terms of β, the radial slope of the deformed plate

$$\kappa_r = \beta', \qquad \kappa_\theta = \beta/r, \qquad \beta = -w'. \tag{5}$$

2.2. EQUATIONS OF MOTION

The equations of infinitesimal motion for the axisymmetric plate deformation considered are

$$\tau_{r,r} + \tau_{rz,z} + (\tau_r - \tau_\theta)/r = \rho\ddot{u}, \tag{6}$$

$$\tau_{rz,r} + \tau_{z,z} + \tau_{rz}/r = \rho\ddot{w}, \tag{7}$$

where ρ is the material density, and dot denotes differentiation with respect to time. Defining plate in-plane stress resultants and transverse shear force, stress couples and inertia terms via

$$(N_r, N_\theta, Q_r) = \int_{-h_1}^{h_2} (\tau_r, \tau_\theta, \tau_{rz})\,\mathrm{d}z, \qquad (M_r, M_z) = \int_{-h_1}^{h_2} (\tau_r, \tau_\theta) z\,\mathrm{d}z.$$

$$(R_0, R_1, R_2) = \int_{-h_1}^{h_2} (1, z, z^2)\rho\,\mathrm{d}z, \tag{8}$$

(where h_1 and h_2 are distances to the bounding plane of the plate) and performing suitable integrations of equations (6) and (7) over the plate thickness, the following dynamical equations are obtained for the annular plates:

$$(rN_r)_{,r} - N_\theta = R_0 r\ddot{u}_0 - R_1 r\ddot{w}_{0,r}, \qquad (rQ_r)_{,r} = R_0 r\ddot{w}_0, \tag{9, 10}$$

$$(rM_r)_{,r} - M_\theta - rQ_r = R_1 r\ddot{u}_0 - R_2 r\ddot{w}_{0,r}. \tag{11}$$

2.3. STRESS–STRAIN RELATIONS

Hooke's law for a polar orthotropic material is written in terms of the elastic stiffness moduli for the plane stress as

$$\begin{bmatrix} \tau_r \\ \tau_\theta \end{bmatrix} = \begin{bmatrix} E_{rr} & E_{r\theta} \\ E_{\theta r} & E_{\theta\theta} \end{bmatrix} \begin{bmatrix} \varepsilon_r \\ \varepsilon_\theta \end{bmatrix}, \tag{12}$$

where the numerical values of the moduli vary from one ply to another. Combining equations (8) and (12) produces the stress–strain relations

$$\begin{bmatrix} N_r \\ N_\theta \\ M_r \\ M_\theta \end{bmatrix} = \begin{bmatrix} A_{rr} & A_{r\theta} & B_{rr} & B_{r\theta} \\ A_{\theta r} & A_{\theta\theta} & B_{\theta r} & B_{\theta\theta} \\ \textit{Symmetric} & & D_{rr} & D_{r\theta} \\ & & D_{\theta r} & D_{\theta\theta} \end{bmatrix} \begin{bmatrix} \varepsilon_{r0} \\ \varepsilon_{\theta 0} \\ \kappa_r \\ \kappa_\theta \end{bmatrix}, \tag{13}$$

where the constants A, B and D are defined by the integrals

$$(A_{ij}, B_{ij}, D_{ij}) = \int_{-h_1}^{h_2} (1, z, z^2) E_{ij}\, \mathrm{d}z \quad (i, j = r, \theta) \tag{14}$$

with the symmetry relation

$$E_{r\theta} = E_{\theta r}. \tag{15}$$

2.4. DISPLACEMENT EQUATIONS OF MOTION

For axisymmetric vibrations of circular frequency λ the displacement field can be expressed in the usual fashion as a product of spatial and time-dependent functions:

$$\begin{aligned} u^{(j)}(r, z, t) &= U^{(j)}(r, z)\mathrm{e}^{\mathrm{i}\lambda t} = [U_0^{(j)}(r) + z\beta_0^{(j)}]\mathrm{e}^{\mathrm{i}\lambda t}, \\ w^{(j)}(r, z, t) &= W^{(j)}(r, z)\mathrm{e}^{\mathrm{i}\lambda t} = W_0^{(j)}(r)\mathrm{e}^{\mathrm{i}\lambda t} \quad (j = I, O), \\ \beta_0^{(j)} &= -W_0^{(j)'}. \end{aligned} \tag{16}$$

Although the superscript describes whether the inner or outer plate is being referred to, the concentric plates are assumed to vibrate as a single structure with the same frequency.

The equations of motion (9)–(11) are then reduced to a set of simultaneous ordinary differential equations in $U_0^{(j)}$ and $W_0^{(j)}$:

$$\begin{aligned} L_{11}^{(j)} U_0^{(j)} + L_{12}^{(j)} W_0^{(j)} &= 0, \\ L_{21}^{(j)} U_0^{(j)} + L_{22}^{(j)} W_0^{(j)} &= 0, \end{aligned} \tag{17}$$

where the differential operators are

$$L_{11}^{(j)} = A_{rr}^{(j)}[(\ )' + r(\ )''] - A_{\theta\theta}^{(j)}(\ )/r + R_0^{(j)}\lambda^2 r(\ ), \tag{18}$$

$$L_{12}^{(j)} = -B_{rr}^{(j)}[r(\ )''' + (\ )''] + B_{\theta\theta}^{(j)}(\ )'/r - R_1^{(j)}\lambda^2 r(\ ), \tag{19}$$

$$L_{21}^{(j)} = B_{rr}^{(j)}[r(\ )''' + 2(\ )''] + B_{\theta\theta}^{(j)}[-(\ )'/r + (\ )/r^2] + R_1^{(j)}\lambda^2[r(\ )' + (\ )], \tag{20}$$

$$L_{22}^{(j)} = -D_{rr}^{(j)}[r(\ )^{iv} + 2(\ )'''] - D_{\theta\theta}^{(j)}[-(\ )''/r + (\ )'/r^2] + R_0^{(j)}\lambda^2 r(\ ) - R_2^{(j)}\lambda^2[r(\ )'' + (\ )']. \tag{21}$$

In these equations the prime denotes differentiation with respect to r. As in equations (16) the superscript j ($= I, O$) in equations (17)–(21) indicates that (a) there will be two sets of equations of motion, for the inner and outer plates, and (b) the plates laminations and densities may be dissimilar. Thus, the four equations (17) must be solved subject to appropriate boundary conditions, as well as matching conditions at the interface between the two concentric plates. The equations can be simplified slightly by neglecting rotatory inertia and choosing a convenient reference plane that eliminates the appearance of terms containing R_1 (see reference [1]).

2.5. BOUNDARY AND MATCHING CONDITIONS

In order to extract the frequency of vibration it is necessary to specify boundary conditions for each of the plates and matching conditions at their interface. A condition of complete restraint is imposed along the circumference of the outer plate $r = a$:

$$U^{(O)}(a) = W^{(O)}(a) = W^{(O)'}(a) = 0. \tag{22}$$

The inner circumference of the inner plate is taken to be clamped so that at $r = b$:

$$U^{(I)}(b) = W^{(I)}(b) = W^{(I)'}(b) = 0. \tag{23}$$

At the interface between the two plates, $r = c$, appropriate matching conditions are imposed:

$$W^{(I)}(c) = W^{(O)}(c), \qquad W^{(I)'}(c) = W^{(O)'}(c), \tag{24, 25}$$

$$M_r^{(I)}(c) = M_r^{(O)}(c), \qquad Q_r^{(I)}(c) = Q_r^{(O)}(c), \tag{26, 27}$$

$$U^{(I)}(c) = U^{(O)}(c), \qquad N_r^{(I)}(c) = N_r^{(O)}(c) \tag{28, 29}$$

in which

$$M_r^{(j)} = B_{rr}^{(j)}U^{(j)'} + B_{r\theta}^{(j)}U^{(j)}/r - D_{rr}^{(j)}W^{(j)''} - D_{r\theta}^{(j)}W^{(j)'}/r, \tag{30}$$

$$Q_r^{(j)} = \partial M_r^{(j)}/\partial r + (M_r^{(j)} - M_\theta^{(j)})/r, \tag{31}$$

$$M_\theta^{(j)} = B_{r\theta}^{(j)}U^{(j)'} + B_{\theta\theta}^{(j)}U^{(j)}/r - D_{r\theta}^{(j)}W^{(j)''} - D_{\theta\theta}^{(j)}W^{(j)'}/r \tag{32}$$

and

$$N_r^{(j)} = A_{rr}^{(j)}U^{(j)'} + A_{r\theta}^{(j)}U^{(j)}/r - B_{rr}^{(j)}W^{(j)''} - B_{r\theta}^{(j)}W^{(j)'}/r. \tag{33}$$

Thus, there are 12 boundary and matching conditions for the two sets of sixth order differential equations, (17), whose eigenvalues are sought.

3. DETERMINATION OF FREQUENCY OF VIBRATION

For the special case of axisymmetric vibrations of concentric isotropic composite plates the simultaneous equations (17) for $U_0^{(j)}$ and $W_0^{(j)}$ reduce to equations (17) of reference [6], where a closed-type solution was given in terms of Bessel functions. For the orthotropic case under consideration here no such solution appears to be available so that a numerical approach for solving the eigenvalue problem must be adopted. A finite difference method is used.

The radial width of the plate, $a - b$, is divided into N equispaced sections of length Δr. Thus, a point at a distance r_i from the origin is defined by

$$r_i = b + i\Delta r, \quad i \in \{0, 1, 2, 3, \ldots, N\} \text{ with } a - b = N\Delta r. \tag{34}$$

It is essential to impose the constraint that Δr is chosen such that the point of interface between the inner and outer plates coincides with an integer value of i, say $N_c\Delta r = c$. Equations (17) are discretized, using fourth order central differences, and replaced by their finite difference approximations at the points corresponding to $i = 1, 2, 3, \ldots (N_c - 1)$, $(N_c + 1), \ldots, (N - 1)$. At $r = a$ and b the values of $(U_0^{(O)}, W_0^{(O)})$ and $(U_0^{(I)}, W_0^{(I)})$ are, respectively, zero (see equations (22) and (23)), and hence the indices $i = 0$ and N do not appear. It is clear that the use of fourth order central difference discretization of the governing equations at the points $i = 1$ and $N - 1$ introduces values of the dependent variables at points that are external to the range $b \leqslant r \leqslant a$. Values of $U_0^{(O)}$ and $W_0^{(O)}$ beyond the outer circumference are expressed in terms of their values at internal points using (a) fourth order shifted backward differences for the derivative boundary condition, namely,

$$W_0^{(O)'} \cong \frac{1}{\Delta r}(\nabla - \tfrac{1}{2}\nabla^2 - \tfrac{1}{6}\nabla^3 - \tfrac{1}{12}\nabla^4) W_{0,N+1}^{(O)} + O(\nabla^5) = 0, \tag{35}$$

where the subscript $N + 1$ borne by $W_0^{(O)}$ refers to its radial location, and (b) one of the governing equations for the outer annulus written at $r = a$ using shifted backward differences. This yields two linear algebraic equations for $(U_{0,N+1}^{(O)}, W_{0,N+1}^{(O)})$ which are readily solved in terms of internal values of the dependent variables. The procedure at the inner circumference for $U_0^{(I)}$ and $W_0^{(I)}$ is identical except that shifted *forward* differences are now appropriate.

The matching conditions at $i = N_c$ must now be applied. For the inner annulus, equations (17) in their discretized form at $i = (N_c - 1)$ introduce the "external" unknowns $U_{0,N_c+1}^{(I)}$ and $W_{0,N_c+1}^{(I)}$ and the values of $U_{0,N_c}^{(I)}$ and $W_{0,N_c}^{(I)}$ ("external" is used here in the sense of $r > c$). For the outer annulus, the discretized equations (17) at $i = (N_c + 1)$ introduce the "external" unknowns $U_{0,N_c-1}^{(O)}$ and $W_{0,N_c-1}^{(O)}$ and the values of $U_{0,N_c}^{(O)}$ and $W_{0,N_c}^{(O)}$ ("external" is used here in the sense of $r < c$). Thus, eight unknown quantities are to be determined in terms of appropriate "internal" values. To achieve this end use is made of the six matching conditions and two governing equations. The derivatives therein are replaced by fourth order shifted forward/backward differences according to whether inner (I) or outer (O) parameters, respectively, are referred to. As a result of this procedure a set of $(2N - 2)$ simultaneous linear algebraic equations is obtained which is written in matrix form as

$$(\mathbf{\Gamma} - \lambda^2\mathbf{I})\mathbf{\Phi} = \mathbf{0}, \tag{36}$$

where $\mathbf{\Gamma}$ and $\mathbf{I}$ are the finite difference coefficients and unity matrices, respectively, and $\mathbf{\Phi}$ contains the values of U_0 and W_0 at the discrete finite difference points. Equation (36) has a non-trival solution if

$$\det(\mathbf{\Gamma} - \lambda^2\mathbf{I}) = \mathbf{0}, \tag{37}$$

TABLE 1

Material properties

Material (abbreviation)	Density ρ ($kg/m^3 \times 10^3$)	E_{rr} ($N/m^2 \times 10^{10}$)	$E_{r\theta}$ ($N/m^2 \times 10^{10}$)	$E_{\theta\theta}$ ($N/m^2 \times 10^{10}$)
Aluminium (AL)	2·595	6·85	1·51	6·85
S-glass epoxy (SGE)	2·002	5·21	0·3	1·18
Boron–aluminium (BA)	2·725	23·39	3·43	14·89
High strength graphite epoxy (HSG)	1·558	12·41	0·28	1·03
PRD 49-III epoxy (PRD)	1·391	7·92	0·12	0·41
Steel (ST)	7·492	20·6	6·8	20·6

so that the problem is reduced to determining the eigenvalues of the matrix $\mathbf{\Gamma}$. This is achieved by utilizing standard computer library sub-routines that are available for this purpose.

The computer code that was developed for the purpose of computing the vibrational frequency of the concentric dissimilar orthotropic composite annular plates in this work was checked by comparison with the analytical results for similar isotropic plates. The comparison yielded information about the reliability of the code and the number of intervals into which the radial co-ordinate had to be sub-divided for accurate predictions. It was found that satisfactory convergence of the results could be achieved using about 50 sub-divisions.

4. NUMERICAL RESULTS AND DISCUSSION

To gain an insight into the way in which geometrical parameters and combinations of dissimilar material lay-ups in the concentric plates can influence the natural frequency of vibration a number of illustrative examples will be presented. Bi-layered and triple-layered structures will be considered. The relevant data pertaining to the properties of the materials examined are listed in Table 1. In all instances to be discussed the total plate thickness will be taken as $h = 1{\cdot}016$ mm whilst the ratio $a/h = 25$. For ease of presentation two concentric annuli comprising materials A, B,… in the inner annulus and X, Y,… in the outer annulus will be referred to as an **A-B,…**; **X-Y,…** combination. Furthermore, the *increase factor* for two concentric annuli is defined as the ratio between the highest and lowest frequencies obtained for all inner and outer material combinations considered.

4.1. BI-LAYERED CONCENTRIC ANNULI; ISOTROPIC + ORTHOTROPIC MATERIAL COMBINATIONS

Initially, two bi-layered concentric annuli comprised of the same isotropic + orthotropic combination of materials are considered. However, the relative thickness of the materials in

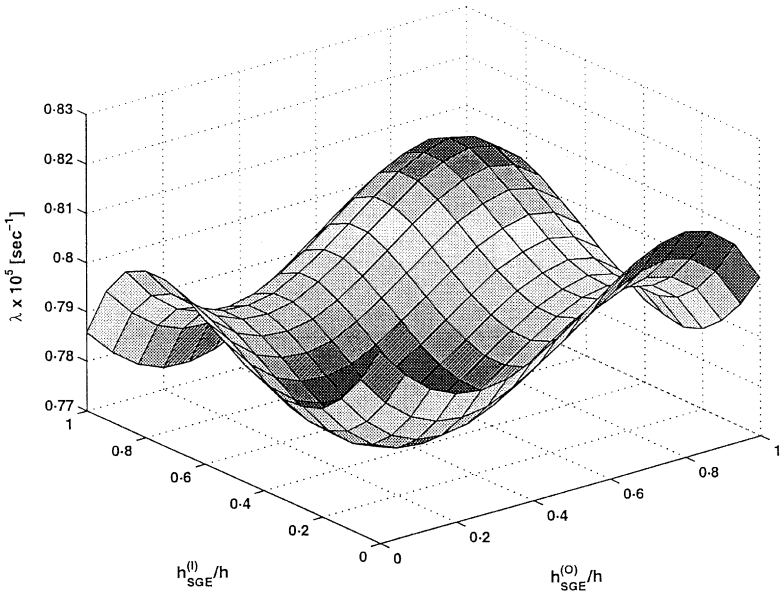

Figure 2. Bi-layered concentric SGE–AL/SGE–AL annuli: variation of the lowest frequency of vibration in phase space of inner and outer annuli's composition: $a/h = 25$, $b/h = 5$, $c/h = 15$.

the two annuli will generally be different. Consider an SGE–AL; SGE–AL combination. To obtain the entire map of the lowest natural frequencies, for a given ratio between the radius of the inner annulus to that of the outer annulus, all possible combinations of relative thickness in both the inner and outer annuli are examined. Thus, for fixed $h_{AL}^{(O)}$ and $h_{SGE}^{(O)}$, $h_{AL}^{(I)}$ and $h_{SGE}^{(I)}$ are varied (keeping the total thickness constant) to cover all combinations of their relative thickness. Then, $h_{AL}^{(O)}$ and $h_{SGE}^{(O)}$ are changed and the inner annulus' layering is varied again following the aforementioned procedure. Further reiteration in this fashion ensures that all material combinations are investigated.

Figure 2 presents a three-dimensional parameter plot showing the frequency of vibration versus the different material combinations. The values of the inner radii of the inner and outer annuli are $b = 5h$ and $c = 15h$ respectively. The map conveys the topographical complexity of the way in which the different material lay-ups in the two annuli influence the natural frequency. Nevertheless, it is found that the increase factor is only about 1·05. For this case the maximum frequency is obtained when the lay-ups in both annuli are identical ($h_{SGE}^{(O)} = h_{SGE}^{(I)} \approx 6h/7$), but the minimum occurs for different inner and outer lay-ups ($h_{SGE}^{(O)} \approx 2h/7$, $h_{SGE}^{(I)} \approx 5h/14$).

In Figure 3 the behaviour of the frequency is drawn as a function of $h_{SGE}^{(O)}/h$ for different values of $h_{SGE}^{(I)}/h$. The shapes of these curves are reminiscent of those obtained by Greenberg and Stavsky [2] for a single orthotropic composite SGE–AL plate. The highest frequency shown on the left-hand side of Figure 3 corresponds to that of a *single* annulus comprised of AL, whereas the lowest frequency on the right-hand side is that of a *single* SGE annulus. The dependency of the frequency on the lay-up in the concentric annuli is evidently non-linear. If a straight line connects the two aforementioned points in Figure 3 it is clear that for a certain range of material arrangements the frequency will be lower than the linear value whereas for the rest of the range it will be higher. Moreover, for each fixed lay-up in the inner annulus altering the outer annulus's lay-up leads to a value of the frequency that transcends the frequency obtained when only SGE or AL are present in the outer annulus.

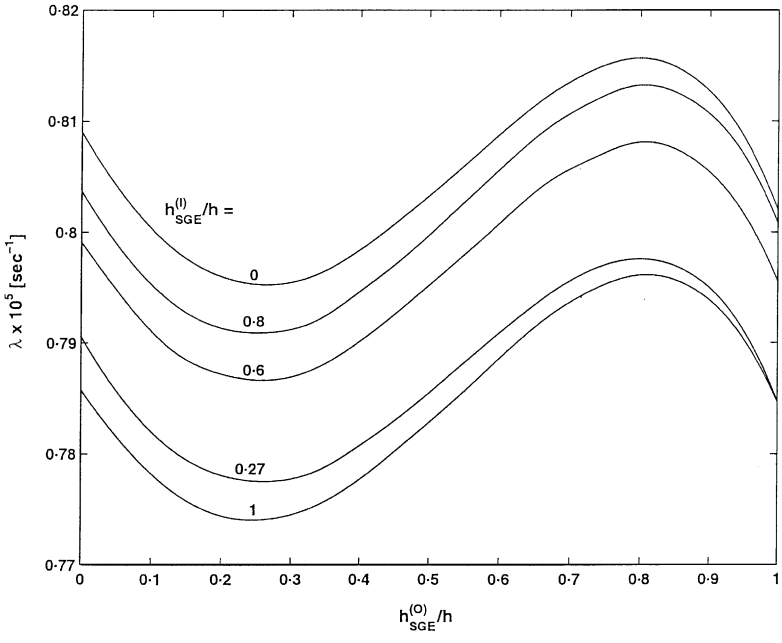

Figure 3. Bi-layered concentric SGE–AL/SGE–AL annuli: variation of the lowest frequency of vibration with composition of outer annulus for different inner annulus compositions: $a/h = 25$, $b/h = 5$, $c/h = 15$.

Interestingly, this maximum occurs when the outer annulus comprises about 80% SGE + 20% AL, irrespective of the make up of the inner annulus. Similarly, a minimum value of the frequency is observed on each curve when the outer annulus contains about 25% SGE + 75% AL. Evidently, the tiering of the outer annulus primarily determines the *shape* of the curves, whereas the inner composition is more dominant for the determination of their *location*. This highlights the roles of *both* the annuli in establishing the vibrational response of the structure.

The effect of the geometry of the two concentric annuli is illustrated in Figures 4(a) and 4(b) where three-dimensional maps are drawn for an HSG–ST/SGE–AL combination. Figures 4(a) and (b) relate to $c/h = 10$ and 20 respectively. The dramatic change in the topography is striking. Furthermore, for $c/h = 10$ the increase factor is 1·07, whereas for $c/h = 20$ it jumps to 1·76.

The way in which the tiering of the annuli influence these results can be seen in Figures 5(a) and 5(b). In Figure 5(a) the frequency is plotted as a function of the inner annulus's lay-up, for the outer annulus's lay-up that yields the overall maximum frequency and for three values of c/h. Figure 5(b) shows the same plots but for the minimum frequency. The importance of the HSG–ST composition of the inner annulus is evidently of prime importance since both the maximum and minimum frequencies increase as c/h increases (i.e., the inner annulus occupies a greater volume of the entire structure than the outer one does). However, it should be noted that the composition of the annuli at which the extrema occur changes with the geometry. For example, when $c/h = 20$ the highest frequency occurs when there is only HSG in the inner annulus and only AL in the outer one, but when $c/h = 15$ the make up is 100% HSG in the inner annulus and 80% SGE + 20% AL in the outer one.

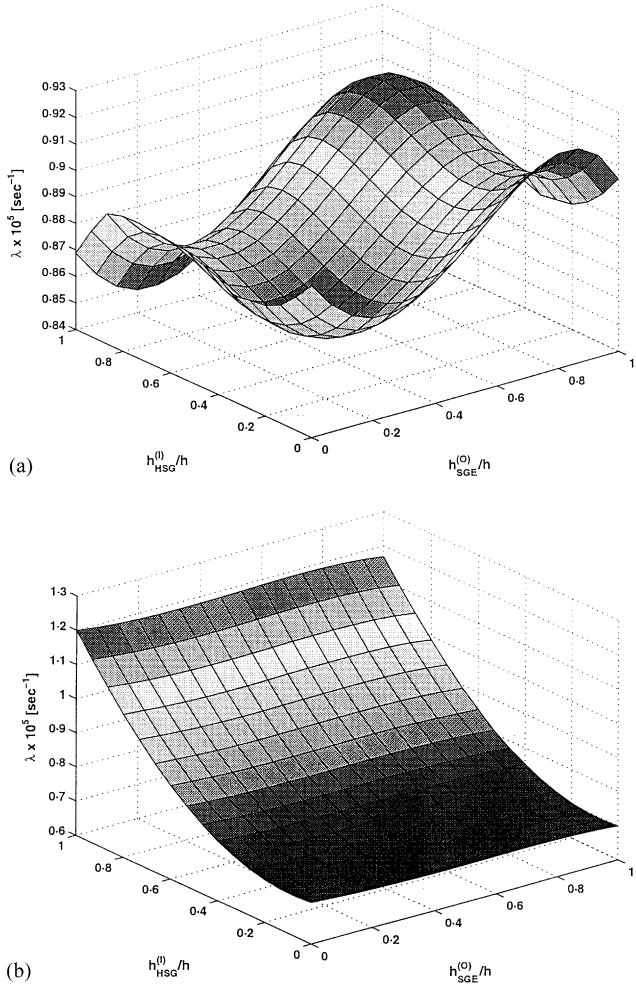

Figure 4. Bi-layered HSG–ST/SGE–AL concentric annuli: influence of c/h on variation of the lowest frequency of vibration in phase space of inner and outer annuli's composition: $a/h = 25$, $b/h = 5$; (a) $c/h = 10$, (b) $c/h = 20$.

4.2. BI-LAYERED CONCENTRIC ANNULI; ORTHOTROPIC + ORTHOTROPIC MATERIAL COMBINATIONS

Two bi-layered concentric annuli comprised of the same orthotropic + orthotropic combination of materials are now considered. However, the relative thickness of the materials in the two annuli will generally be different. In Figure 6 a three-dimensional parameter is shown for an HSG–BA/HSG–BA combination. Comparison of Figure 6 with Figure 2 reveals some qualitative topographical similarity. However, the current material set-up exhibits higher frequencies and a more curved shape, the latter presumably due to the wider *range* of natural frequencies involved. Indeed, the increase factor is found to be approximately 1·1.

In Figure 7, the dependence of the frequency on the inner annulus composition is shown for different outer annulus composition and for $c/h = 20$. Also drawn (as a broken line), for comparative purposes, is the frequency response of a *single* HSG–BA annulus ($a/h = 25$, $b/h = 5$) as a function of composition. Some points should be noted. (a) The curves for the

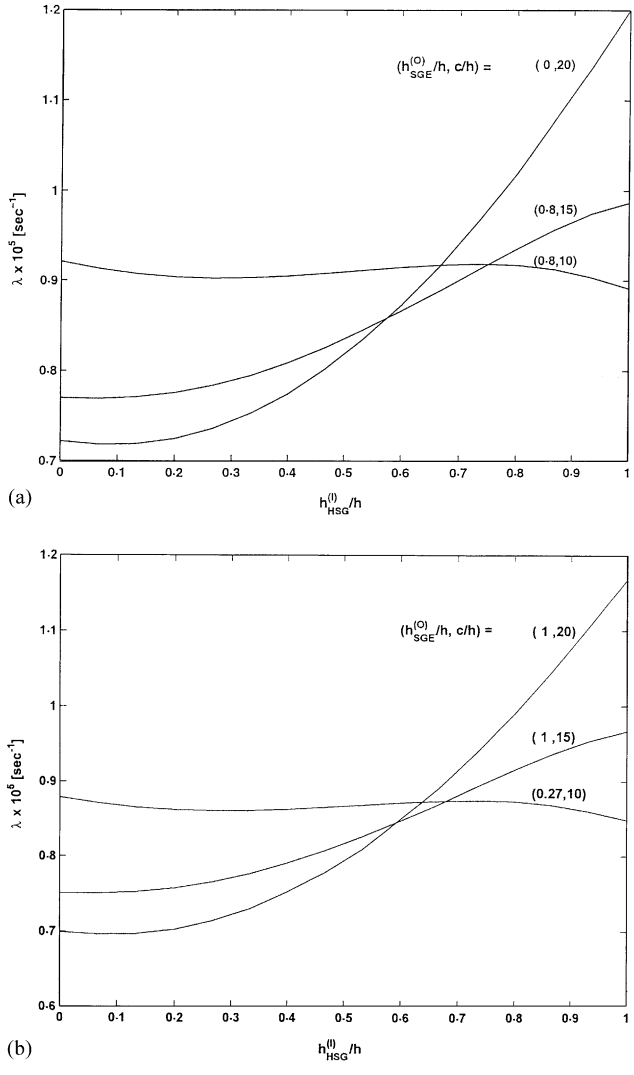

Figure 5. Bi-layered HSG–ST/SGE–AL concentric annuli: variation of lowest frequency of vibration with composition of inner annulus and annulus geometry for (a) outer annulus lay-up that yields the overall maximum frequency and (b) outer annulus lay-up that yields the overall maximum frequency.

concentric annuli manifest a behaviour that is similar to that of the single annulus. The increase factor for the latter is about 1·1. A close examination of all the data (including that not shown in Figure 7) reveals that the increase factor for the concentric annuli is 1·18. Thus, in the present case, use of two annuli results in a relatively mild advantage in terms of the frequency in comparison with the use of a single annulus. (b) Comparison of the concentric annuli curves for different outer compositions discloses the "wave-like" response of the frequency to the inner annulus composition. Interestingly, the lower extrema on the curves occur at approximately the same inner composition of $h^{(I)}_{HSG}/h \approx 0{\cdot}3$–$0{\cdot}34$ whilst the upper extrema occur at $h^{(I)}_{HSG}/h \approx 0{\cdot}8$–$0{\cdot}84$, irrespective of the outer annulus composition. Qualitatively, this is reminiscent of the behaviour described earlier for the SGE–AL/SGE–AL combinations (see Figure 3).

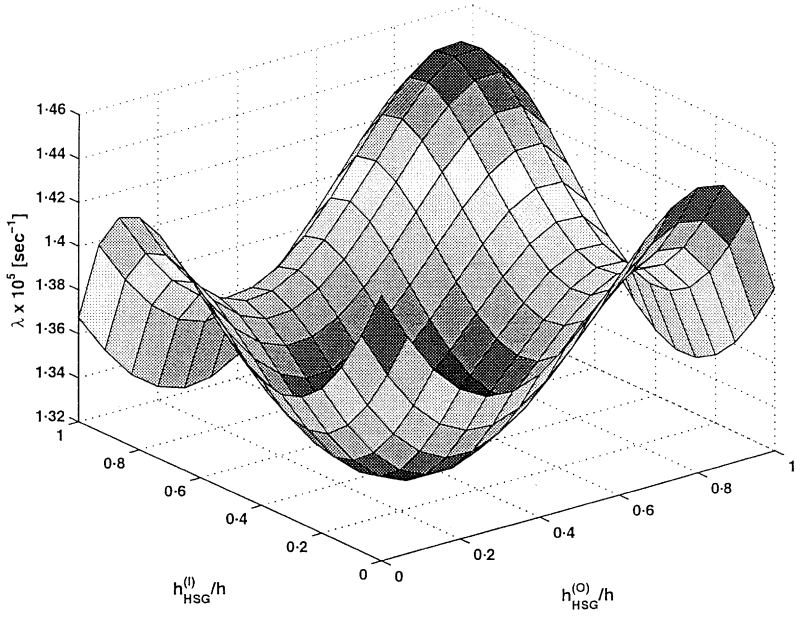

Figure 6. Bi-layered concentric HSG–BA/HSG–BA annuli: variation of the lowest frequency of vibration in phase space of inner and outer annuli's composition: $a/h = 25$, $b/h = 5$, $c/h = 15$.

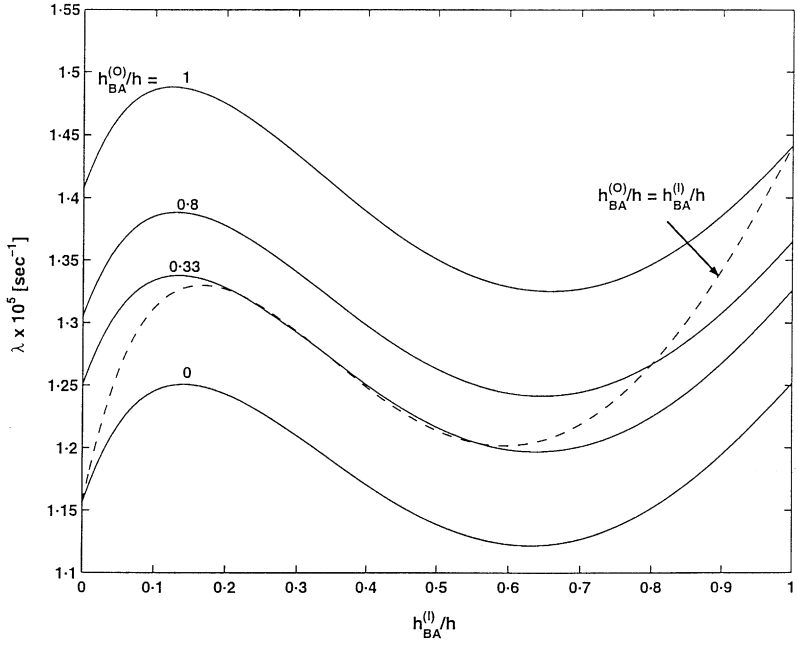

Figure 7. Bi-layered concentric HSG–BA/HSG–BA annuli: variation of the lowest frequency of vibration variation with composition of inner annulus for different outer annulus composition; broken line is curve for a single HSG–BA annulus: $a/h = 25$, $b/h = 5$, $c/h = 20$.

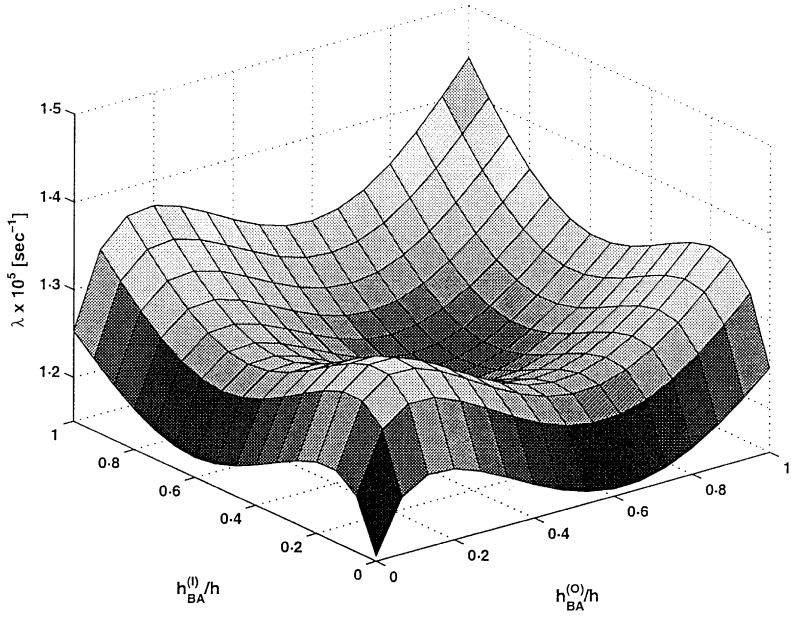

Figure 8. Bi-layered concentric BA–PRD/BA–PRD annuli: variation of the lowest frequency of vibration in phase space of inner and outer annulus composition: $a/h = 25$, $b/h = 5$, $c/h = 15$.

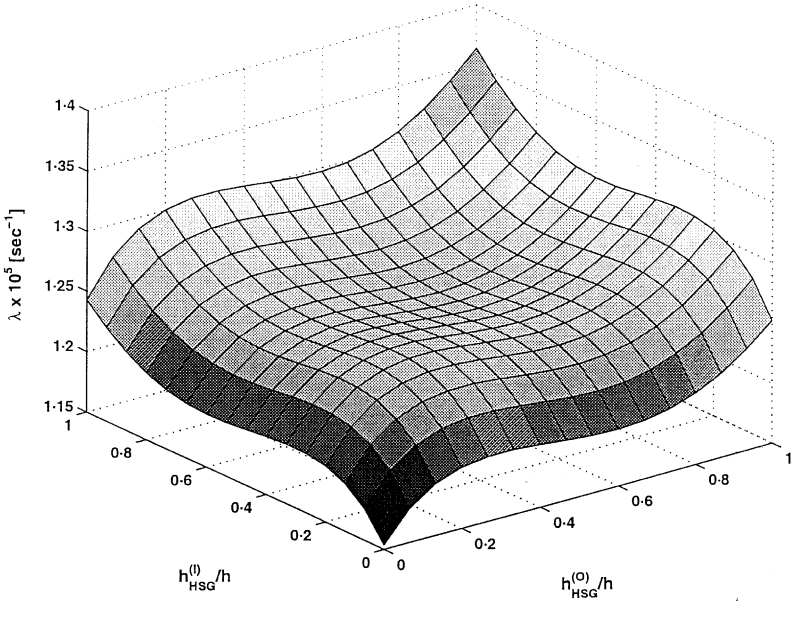

Figure 9. Bi-layered concentric HSG–PRD/HSG–PRD annuli: variation of the lowest frequency of vibration in phase space of inner and outer annuli's composition: $a/h = 25$, $b/h = 5$, $c/h = 15$.

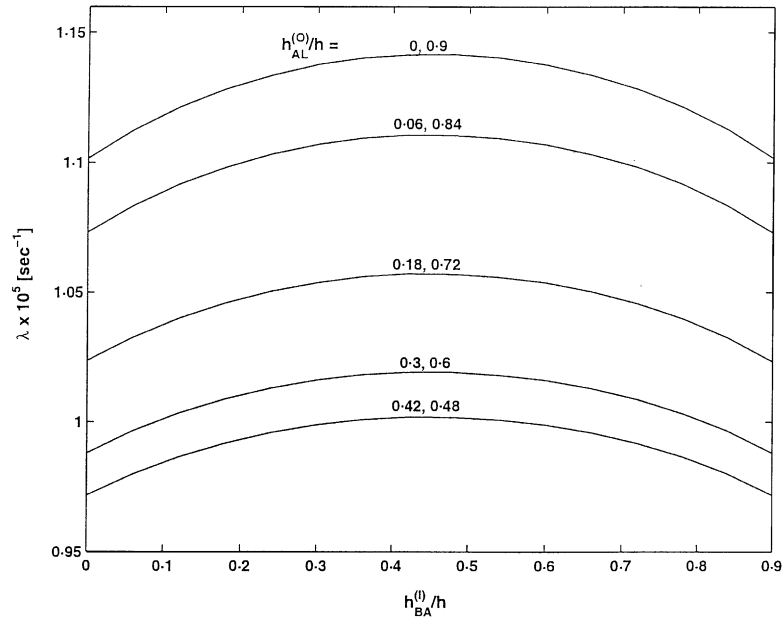

Figure 10. Triple-layered concentric BA–AL–BA/AL–BA–AL annuli: variation of the lowest frequency of vibration with composition of inner annulus for varying outer annulus composition: $a/h = 25$, $b/h = 5$, $c/h = 15$.

A three-dimensional parameter plot is drawn for a BA–PRD/BA–PRD combination in Figure 8. The topography is notably different to that in Figure 6 and there is a 4% growth in the increase factor, to 1·14. The maximum frequency occurs when BA occupies 100% of both the inner and outer annuli, i.e., for a single-layered BA annulus. Conversely, the minimum frequency is found for a single PRD annulus.

Figure 9 illustrates the three-dimensional plot for an HSG–PRD/HSG–PRD combination. The topography has flattened out considerably in comparison with Figures 6 and 8, and only mild extrema are visible. The increase factor for this combination is found to be about 1·1. Now, the maximum frequency is found for a single HSG annulus, whereas the minimum frequency is supplied by a single PRD annulus. Although no clear-cut, simple rule of thumb emerges from these results it is of interest to observe that of the three materials considered in Figures 8 and 9 the one with the smallest orthotropy ratio, $E_{\theta\theta}/E_{rr}$, is PRD having a value of 0·0518. The values for BA and HSG are 0·6369 and 0·083, respectively, and the maximum frequencies that are found for BA and HSG single annuli (see Figures 8 and 9) obey the inequality $\lambda_{BA} > \lambda_{HSG}$. However, the non-linear frequency response to the inner and outer annulus composition, evident from Figures 6, 8 and 9 underscores the subtle, non-trivial way in which the orthotropy of the materials in the annuli influence the vibrational response.

4.3. TRIPLE-LAYERED CONCENTRIC ANNULI

Suppose each of the concentric annuli is comprised of an upper and lower layer (not necessarily of the same material) glued to a core of a different material. The total thickness of the structure is maintained constant, as is the core thickness that is fixed at $0{\cdot}1h$. The relative thickness of the upper and lower layers in both the inner and outer annuli is varied to generate the entire frequency response for all material combinations.

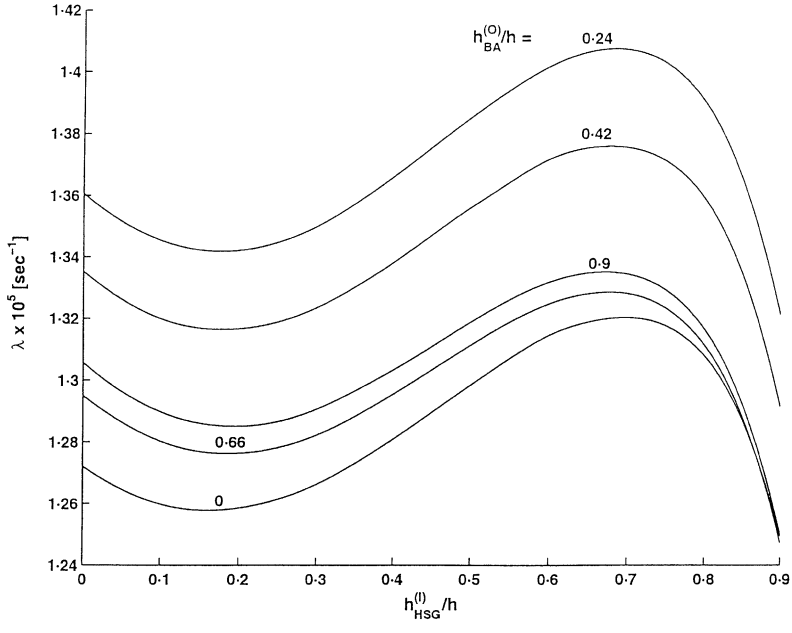

Figure 11. Triple-layered concentric HSG–AL–BA/BA–AL–HSG annuli: variation of the lowest frequency of vibration composition of inner annulus for varying outer annulus composition: $a/h = 25$, $b/h = 5$, $c/h = 15$.

Consider a BA–AL–BA/AL–BA–AL combination. In Figure 10 the natural frequency is plotted against the inner annulus composition, as the outer composition is varied. The pairs of numbers on each curve indicate the relative thickness of AL in the upper and lower layers in the outer annulus. The curves are symmetric, as expected, with each possessing a maximum for the symmetrically layered inner annulus. The maximum frequency for all material combinations is found when the outer annulus is bi-layered. The increase factor is approximately 1·14.

Now consider an HSG–AL–BA/BA–AL–HSG combination. The relevant frequency plot shown in Figure 11 is different from that of Figure 10. The extrema previously observed in the bi-layered combinations reappear here. The maximum point on each curve occurs when there is about 70% HSG + 10% AL + 20% BA in the inner annulus, irrespective of the outer annulus composition. A similar remark is applicable to the minimum point on each curve (15% HSG + 10% AL + 75% BA). Furthermore, for a fixed inner composition, the frequency does not behave monotonically with the outer annulus composition. The lower and upper curves shown correspond to outer compositions of 10% AL + 90% HSG and 24% BA + 10% AL + 66% HSG respectively. For $h_{BA}^{(O)}/h > 0{\cdot}24$ a "wave-like" behaviour is observed as the outer composition is altered. Despite the qualitative differences between the curves in Figures 10 and 11 the increase factor for the three material case is roughly the same, 1·14, as for the BA–AL–BA/AL–BA–AL combination. However, in quantitative terms the HSG–AL–BA/BA–AL–HSG combination manifests higher frequencies.

4.4. BI- + TRIPLE-LAYERED CONCENTRIC ANNULI

Consider a bi-layered HSG–BA inner annulus surrounded by a triple-layered BA–HSG–BA outer annulus. A three-dimensional parameter plot is drawn in Figure 12 for

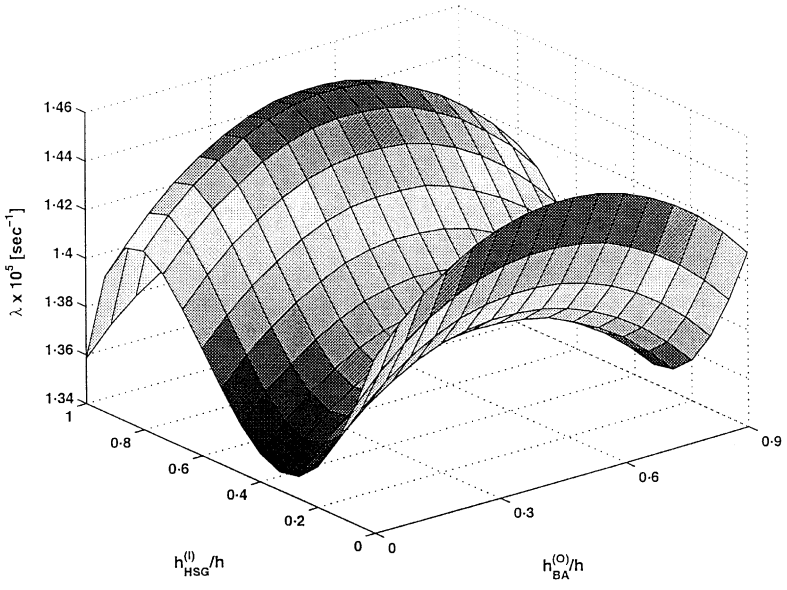

Figure 12. Bi-+triple-layered concentric HSG–BA/BA–HSG–BA annuli: variation of the lowest frequency of vibration in phase space of inner and outer annuli's composition: $a/h = 25$, $b/h = 5$, $c/h = 15$.

this combination. It is instructive to compare this figure to Figure 7 which illustrates the phase plane plot for bi-layered HSG–BA concentric annuli. The topologies of the two surfaces are quite different, once again indicating the extreme sensitivity of the frequency to the layering of the two annuli. Nevertheless, the highest frequencies attained are rather close, of the order of $1{\cdot}45 - 1{\cdot}46 \times 10^5\,\mathrm{s}^{-1}$, as are the increase factors (1·08 for the bi-+triple-layered annuli as compared to 1·1 for the bi-layered annuli). Thus, for the geometry and material lay-ups considered here it seems that there is little to be gained by encompassing the inner annulus with a triple-layered outer annulus.

5. CONCLUSIONS

An analysis of the vibrational behaviour of two concentric dissimilar orthotropic annuli has been presented. The governing field equations were solved numerically using a fourth order finite differences method. Bi-layered triple-layered and bi-+triple-layered material compositions were considered. Computed results for a wide range of possible orthotropic material combinations does not indicate any simple rule of thumb formula for estimating the effect of the material composition on the frequency. However, in keeping with previous results [7] for concentric dissimilar *isotropic* annuli the geometry (expressed via the radii of the inner and outer annuli) was found to have a considerable influence on the natural frequency of vibration. In the absence of appropriate analytical expressions, optimization and, thereby, control of the natural frequency of composite plate-like structures, through geometry and material composition, must make use of parametric studies similar to the current one.

ACKNOWLEDGMENTS

The work of Y. Stavsky was supported in part by the Swope Chair of Mechanics and the Technion Fund for the Promotion of Research. The work of J. B. Greenberg was partially

supported by the Lady Davis Chair in Aerospace Engineering. The technical assistance of M. Mor is gratefully acknowledged.

REFERENCES

1. Y. STAVSKY and R. LOEWY 1971 *Journal of Acoustical Society of America* **49**, 1542–1550. Vibrations of isotropic composite circular plates.
2. J. B. GREENBERG and Y. STAVSKY 1978 *Journal of Sound and Vibration* **61**, 531–545. Axisymmetric vibrations of orthotropic composite circular plates.
3. C.-C. LIN and C.-S. TSENG 1998 *Journal of Sound and Vibration* **209**, 797–810. Free vibration of polar orthotropic laminated circular and annular plates.
4. Y. FROSTIG and G. J. SIMITSES 1986 *Computers and Structures* **24**, 443–454. Buckling of multi-annular plates.
5. H. P. LEE 1992 *Computers and Structures* **43**, 635–644. Buckling of annular plates with stepped variation in thickness.
6. D. G. GORMAN 1983 *Journal of Sound and Vibration* **86**, 47–60. Natural frequencies of transverse vibration of polar orthotropic variable thickness annular plates.
7. J. B. GREENBERG and Y. STAVSKY 1999 *Composites*: *Part B* **30**, 553–567. Axisymmetric vibrations of concentric dissimilar isotropic composite plates.